"Temperature-dependent Studies of Niccolite Metal Formate Frameworks $[(CH_3)_2NH_2][Fe^{III}M^{II}(HCOO)_6]$ (M=Fe and Mg): Structural, Magnetic, Dielectric and Phonon Properties"

by Aneta Ciupa et al.

Table S1. Crystal data, data collection and refinement results for DMFeMg at 298, 190, and 100 K.

For all structures: $C_8H_{14}FeMgNO_{12}$, M_r = 396.36, trigonal, $P\bar{3}1c$, Z = 2. Experiments were carried out with Mo $K\alpha$ radiation. Refinement was with 17 restraints. H-atom parameters were constrained.

Crystal data			
Temperature (K)	298	190	100
a, c (Å)	8.2076(2), 13.8988(6)	8.2067(2), 13.8818(6)	8.2008(2), 13.8667(6)
V (Å^3)	810.85 (5)	809.68 (5)	807.64 (5)
μ (mm^{-1})	1.03	1.03	1.03
Crystal size (mm)	0.22 × 0.11 × 0.10	0.22 × 0.11 × 0.10	0.22 × 0.11 × 0.10
Data collection			
T_{min}, T_{max}	0.989, 1.000	0.927, 1.000	0.927, 1.000
No. of measured, independent and observed [$I > 2\sigma(I)$] reflections	8337, 518, 433	7770, 517, 451	7668, 516, 429
R_{int}	0.037	0.026	0.036
$(\sin\theta/\lambda)_{max}$ (Å^{-1})	0.609	0.609	0.610
Refinement			
$R[F^2 > 2\sigma(F^2)]$, $wR(F^2)$, S	0.024, 0.062, 1.19	0.024, 0.068, 1.02	0.027, 0.089, 0.95
No. of reflections	518	517	516

No. of parameters	44	46	44
$\Delta\rho_{max}$, $\Delta\rho_{min}$ (e Å^{-3})	0.30, -0.28	0.44, -0.26	0.58, -0.33

Computer programs: *CrysAlis PRO*, Oxford Diffraction Ltd., Version 1.171.33.42 (release 29-05-2009 CrysAlis171 .NET) (compiled May 29 2009,17:40:42), *SHELXL2014*/7 (Sheldrick, 2014), Diamond Version 3.2k Crystal Impact GbR, Bonn, Germany.

Table S2. The correlation diagram showing the correspondence between the optical modes in the $P\bar{3}1c$ and $R\bar{3}c$ structures of DMFeFe (the data for the $R\bar{3}c$ structure are given in parentheses).

ion	vibration	Free ion symmetry	Site symmetry	Factor group symmetry
HCOO-		**C_{2v}**	**C_1 (C_1)**	**D_{3d} (D_{3d})**
	ν_1, ν_2 or ν_3	A_1	A (3A)	$A_{1g}+A_{2g}+2E_g+A_{1u}+A_{2u}+2E_u$ ($3A_{1g}+3A_{2g}+6E_g+3A_{1u}+3A_{2u}+6E_u$)
	ν_4, ν_5 or ν_6	B_1	A (3A)	$A_{1g}+A_{2g}+2E_g+A_{1u}+A_{2u}+2E_u$ ($3A_{1g}+3A_{2g}+6E_g+3A_{1u}+3A_{2u}+6E_u$)
	T’	$A_1 + B_1 + B_2$	3A (9A)	$3A_{1g}+3A_{2g}+6E_g+3A_{1u}+3A_{2u}+6E_u$ ($9A_{1g}+9A_{2g}+18E_g+9A_{1u}+9A_{2u}+18E_u$)
	L	$A_2 + B_1 + B_2$	3A (9A)	$3A_{1g}+3A_{2g}+6E_g+3A_{1u}+3A_{2u}+6E_u$ ($9A_{1g}+9A_{2g}+18E_g+9A_{1u}+9A_{2u}+18E_u$)
DMA^+		**C_{2v}**	**C_2 (C_2)**	**D_{3d} (D_{3d})**
	$\nu_s(NH_2)$	A_1	A (A)	($3A_{1g}+3A_{1u}$)
	$\nu_{as}(NH_2)$	B_2	B (B)	($3A_{2g}+3A_{2u}$)
	$\delta(NH_2)$	A_1	A (A)	($3A_{1g}+3A_{1u}$)
	$\rho(NH_2)$	B_2	B (B)	($3A_{2g}+3A_{2u}$)
	$\omega(NH_2)$	B_1	B (B)	($3A_{2g}+3A_{2u}$)
	$\tau(NH_2)$	A_2	A (A)	($3A_{1g}+3A_{1u}$)
	ν_s(CNC)	A_1	A (A)	($3A_{1g}+3A_{1u}$)

	ν_{as}(CNC)	B_1	B (B)	$(3A_{2g}+3A_{2u})$
	δ(CNC)	A_1	A (A)	$(3A_{1g}+3A_{1u})$
	$\nu_s(CH_3)$	A_1+B_1	A+B (A+B)	$A_{1g}+A_{2g}+A_{1u}+A_{2u}$ $(3A_{1g}+3A_{2g}+3A_{1u}+3A_{2u})$
	$\nu_{as}(CH_3)$	$A_1+B_1+B_2+A_2$	2A+2B (2A+2B)	$2E_g+2E_u$ $(6E_g+6E_u)$
	$\delta_s(CH_3)$	A_1+B_1	A+B (A+B)	$A_{1g}+A_{2g}+A_{1u}+A_{2u}$ $(3A_{1g}+3A_{2g}+3A_{1u}+3A_{2u})$
	$\delta_{as}(CH_3)$	$A_1+B_1+B_2+A_2$	2A+2B (2A+2B)	$2E_g+2E_u$ $(6E_g+6E_u)$
	$\rho(CH_3)$	$A_1+B_1+B_2+A_2$	2A+2B (2A+2B)	$2E_g+2E_u$ $(6E_g+6E_u)$
	$\tau(CH_3)$	A_2+B_2	A+B (A+B)	$A_{1g}+A_{2g}+A_{1u}+A_{2u}$ $(3A_{1g}+3A_{2g}+3A_{1u}+3A_{2u})$
	T’	$A_1+B_1+B_2$	A+2B (A+2B)	$(A_{1g}+2A_{2g}+A_{1u}+2A_{2u}+3E_g+3E_u)$
	L	$A_2+B_1+B_2$	A+2B (A+2B)	$(A_{1g}+2A_{2g}+A_{1u}+2A_{2u}+3E_g+3E_u)$
Fe^{2+}			**D_3 (C_2)**	**D_{3d} (D_{3d})**
			A_2 (A)	$A_{2u}+A_{2g}$ $(A_{1g}+A_{1u}+E_g+E_u)$
			E (2B)	E_g+E_u $(2A_{2g}+2A_{2u}+2E_g+2E_u)$
Fe^{3+}			**S_6 (S_6+ C_3)**	**D_{3d} (D_{3d})**
			A_u (A_u+A)	$A_{1u}+A_{2u}$ $(A_{1g}+A_{2g}+2A_{1u}+2A_{2u})$
			E_u (E_u+E)	E_u $(2E_g+4E_u)$

Table S3. IR and Raman frequencies (in cm^{-1}) of DMFeFe and suggested assignments.[a]

Raman				IR		Assignment
y(xx)y	y(zz)y	y(xz)y	z(xy)z			
$A_{1g}+E_g$	A_{1g}	E_g	E_g	297 K	4 K	
				3167w	3188w	$\nu(NH_2)$
3122w				3109w	3089w	$\nu(NH_2)$
3044m			3044w	3045vw	3046w	$\nu_{as}(CH_3)$
					3009w	overtone
3035m	3035w	3033w	3035w	3037vw	3043w	$\nu_{as}(CH_3)$
2972s	2972s	2973vw	2972w	2974w	2979sh, 2974w	$\nu_{s(}CH_3)$
2877s	2876w	2878w	2878m	2882w, 2873w	2884w, 2876w	$\nu_1(HCOO^-)$
2825w	2825vw					overtone
2763w				2766w		$2\nu_2(HCOO^-)$
2727w						$2\nu_2(HCOO^-)$
1671s	1671s	1667w	1671w			ν(C-O)
					1647w	$\delta(NH_2)$
1566w		1575w	1565w	1589vs	1613sh, 1595vs	$\nu_4(HCOO^-)$
					1586s, 1574w	
				1471w	1475w	$\delta_{as}(CH_3)$

1457w	1458w	1464w	1457w	1463w	1464w	$\delta_s(CH_3)$
				1452w	1450w, 1446sh	$\delta_{as}(CH_3)$
				1445sh		$\delta_{as}(CH_3)$
				1405sh	1402sh	$\nu_5(HCOO^-)$
1386s	1386s	1386s	1386s	1391sh, 1383m	1397m, 1388m	$\nu_5(HCOO^-)$
1364s	1364s		1364w		1368w	$\nu_2(HCOO^-)$
					1360m	$\nu_2(HCOO^-)$
				1348s	1348s	$\nu_2(HCOO^-)$
1341w	1335w	1337s	1340s	1334sh	1337s	$\nu_2(HCOO^-)$
				1254vw	1258w	$\rho(CH_3)$
					1233vw	$\rho(CH_3)$
		1081vw	1083w	1084w	1084w	$\rho(CH_3)$
1064vw		1064vw	1064w	1065vw	1069vw, 1064vw	$\nu_6(HCOO^-)$
				1031w	1027w	$\rho(CH_3)$
		1013vw	1013vw	1014w	1016w	$\nu_{as}(CNC)$
881w	881s		880vw	883w	886w	$\nu_s(CNC)$
				853w	858w	$\rho(NH_2)$
812m	811w			815s	820s	$\nu_3(HCOO^-)$
		804vw	806w		814sh	$\nu_3(HCOO^-)$
393s	394s	393vw	394w			$\delta(CNC)$
				364s	378s	T'(Fe)
				341sh	348m, 333w	T'(Fe)
		316w	309vw			$\tau(CH_3)$
				296w	299w	T'(Fe) and T'($HCOO^-$)
280w		281w	280w	272w, 264sh	277w, 270w	T'($HCOO^-$)

253w			255w			T’($HCOO^-$)
239w	227w	245w		244w	255w, 246w	T’($HCOO^-$)
				194m	205sh, 201m	T’($HCOO^-$)
				185m	190m	L($HCOO^-$)
180m	173sh			176m	178m, 166w	L($HCOO^-$)
141s	146s		138m			L($HCOO^-$)
		122m				L($HCOO^-$)
105w			106m	109w	133w, 108w, 99w	L(DMA)
68w		66w	69w			T’(DMA)

[a]Key: s, strong; m, medium; w, weak; vw, very weak; sh, shoulder

Table S4. IR and Raman frequencies (in cm^{-1}) of DMFeMg and suggested assignments.[a]

Raman				IR		Assignment
y(xx)y	y(zz)y	y(xz)y	z(xy)z			
$A_{1g}+E_g$	A_{1g}	E_g	E_g	297 K	4 K	
				3170w	3149w, 3130w	$\nu(NH_2)$
3131w				3108w	3091w	$\nu(NH_2)$
3043m			3043w	3044vw	3048w	$\nu_{as}(CH_3)$
3036m	3035w	3035w	3036w	3037vw	3032w	$\nu_{as}(CH_3)$
				2994w	2995w	overtone
2973s	2972s	2972w	2973m	2975w	2973w	$\nu_{s(}CH_3)$
2882s	2878w	2882w	2882m	2884w	2890w, 2882w	$\nu_1(HCOO^-)$
2828w	2825w		2824vw			overtone
				2792w	2807w, 2796w	overtone
				2779w	2787w	$2\nu_2(HCOO^-)$
2767w		2767vw	2769vw			$2\nu_2(HCOO^-)$
2726w						$2\nu_2(HCOO^-)$
1680s	1680s	1670w	1677w			ν(C-O)
1652w					1646w	$\delta(NH_2)$
1571w	1608w	1622w	1570w	1604vs	1633sh, 1611vs	$\nu_4(HCOO^-)$
		1582w			1602sh, 1589sh	

				1471w	1476w	$\delta_{as}(CH_3)$
1457w	1458w	1463w	1459w	1463w	1465w, 1461sh	$\delta_{s}(CH_3)$
				1455w	1451w	$\delta_{as}(CH_3)$
				1444w	1445vw	$\delta_{as}(CH_3)$
1417w			1417vw			$\tau(NH_2)$
				1403sh	1401w	$\nu_5(HCOO^-)$
1388s	1388s	1389s	1390s	1389m	1393m, 1388sh	$\nu_5(HCOO^-)$
1365s	1365s	1365w	1364w	1368w	1367w	$\nu_2(HCOO^-)$
				1357sh	1360w	$\nu_2(HCOO^-)$
				1348s	1349s	$\nu_2(HCOO^-)$
1341w	1334w	1334s	1336m	1338s	1339m	$\nu_2(HCOO^-)$
1252vw				1254vw	1260w	$\rho(CH_3)$
1233w					1231vw	$\rho(CH_3)$
1079vw		1081w	1082vw	1085w	1084w	$\rho(CH_3)$
1067w	1067vw	1066w	1067vw	1067w	1071w	$\nu_6(HCOO^-)$
				1027w	1028w	$\rho(CH_3)$
		1012w	1013vw	1014w	1016w	$\nu_{as}(CNC)$
881w	881s		882w	884vw	886vw	$\nu_{s}(CNC)$
				855w	864w	$\rho(NH_2)$
812m	814w		813w	816s	823s	$\nu_3(HCOO^-)$
		808w	807w		817sh	$\nu_3(HCOO^-)$
391s	389s		392w			$\delta(CNC)$
				379s	396s	T'(Fe,Mg)
		356w	350w	357sh	364m, 348w	T'(Fe,Mg)
280w		282w	279w	274w	272w	$T'(HCOO^-)$
254sh		251w	245w	248w	252w	$T'(HCOO^-)$

238m	231m					T'($HCOO^-$)
			199w	196m	204m, 189m	T'($HCOO^-$)
198m	201m					L($HCOO^-$)
148s	152s		146m			L($HCOO^-$)
		134s				L($HCOO^-$)
106w		106s	104m	108w	133w, 108w	L($HCOO^-$) and L(DMA)
					103vw	
		72w	73w			T'(DMA)

[a]Key: s, strong; m, medium; w, weak; vw, very weak; sh, shoulder

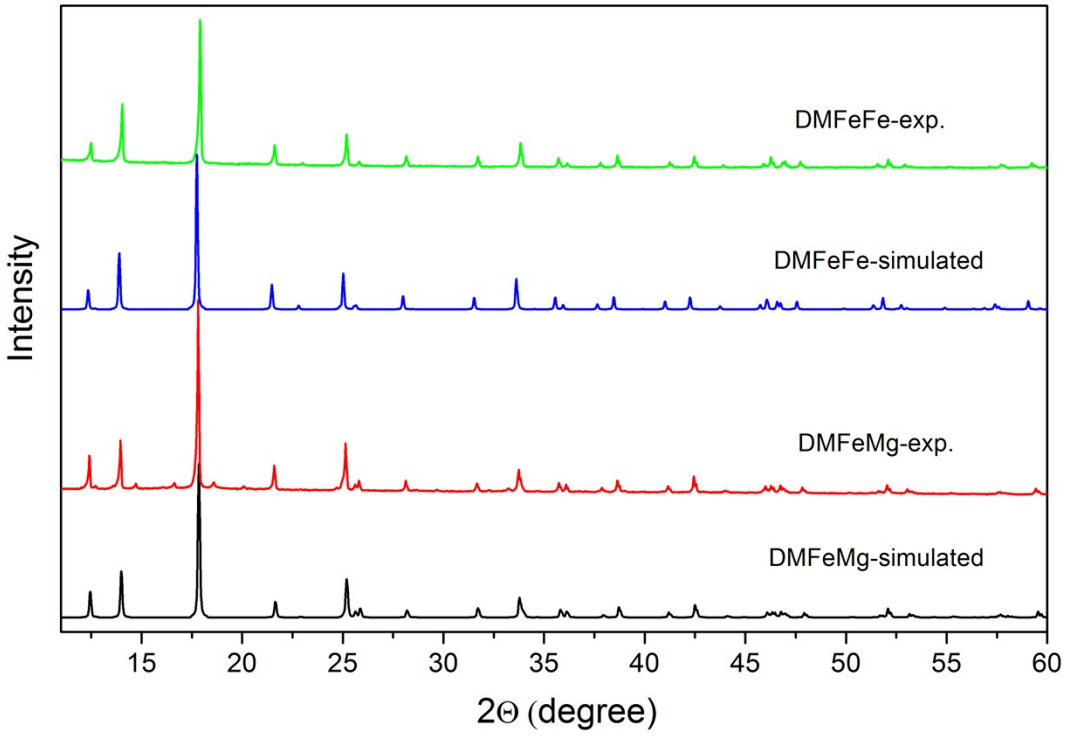

Figure S1. Powder XRD patterns for the as-prepared bulk samples of DMFeFe and DMFeMg, with the calculated ones based on the single crystal structures at 293 K (for DMFeFe taken from Ref. 12 .

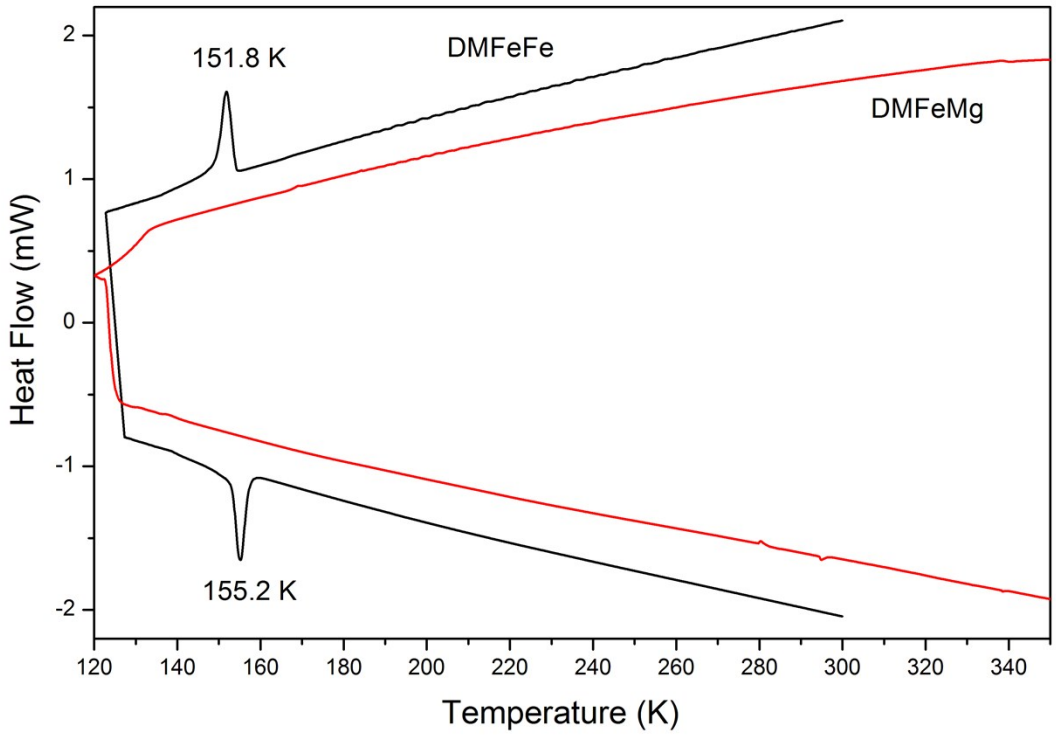

Figure S2. DSC traces for DMFeMg (red) and DMFeFe (black).

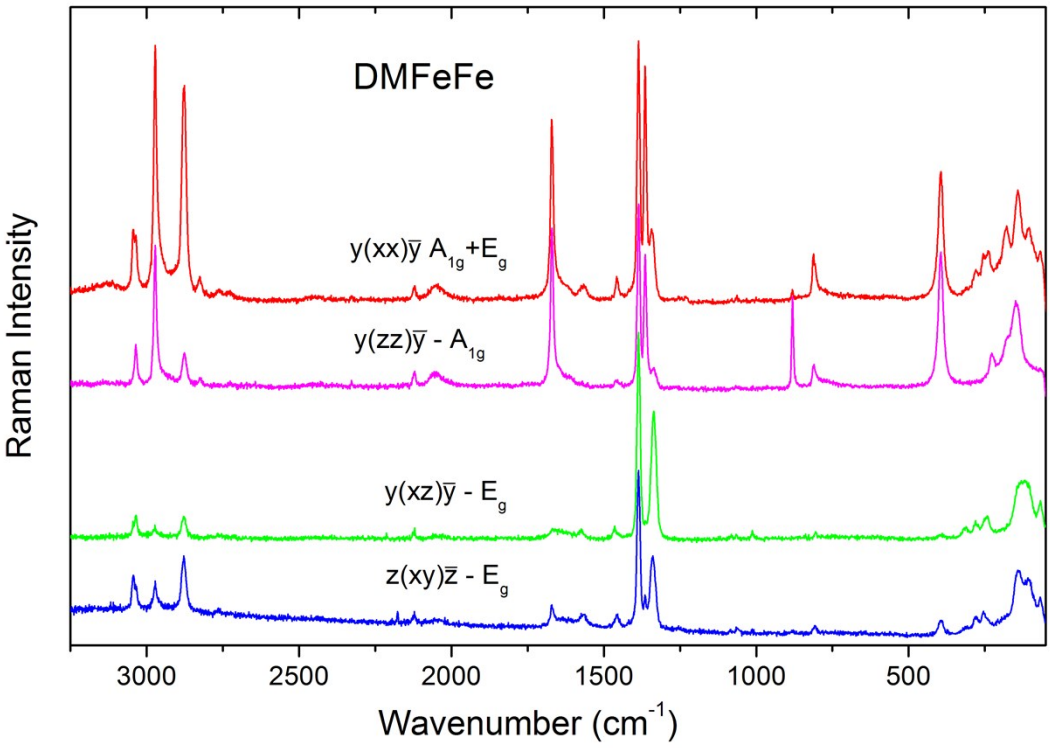

Figure S3. Room-temperature polarized Raman spectra of DMFeFe corresponding to the whole spectral range 50-3250 cm^{-1}.

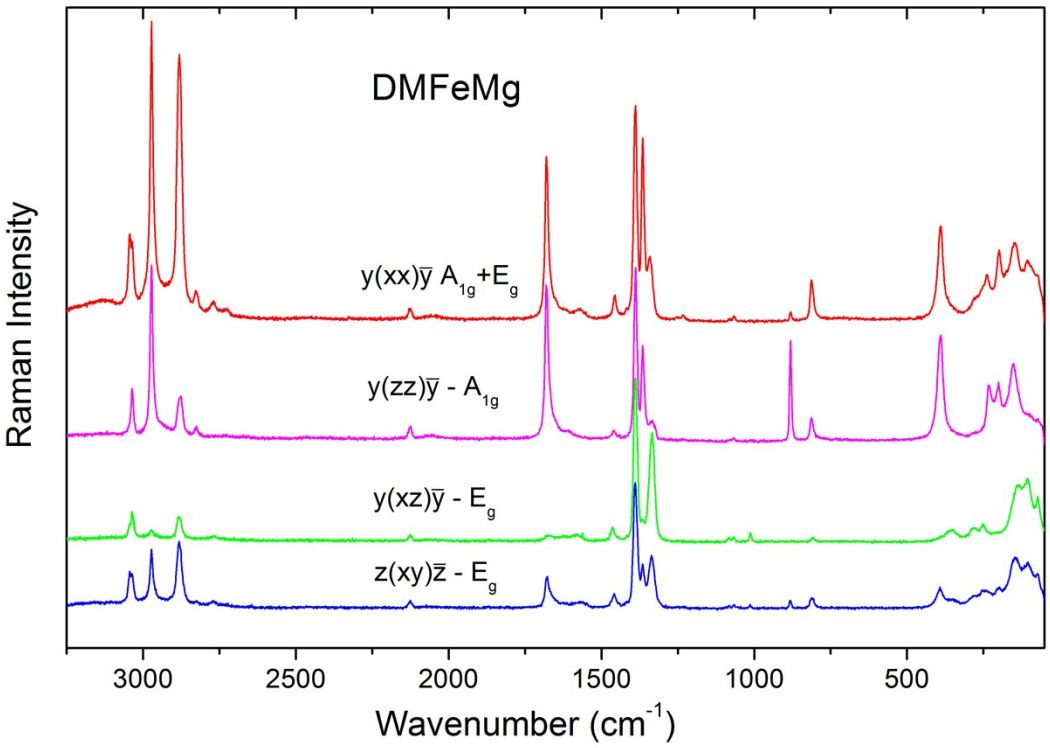

Figure S4. Room-temperature polarized Raman spectra of DMFeMg corresponding to the whole spectral range 50-3250 cm^{-1}.

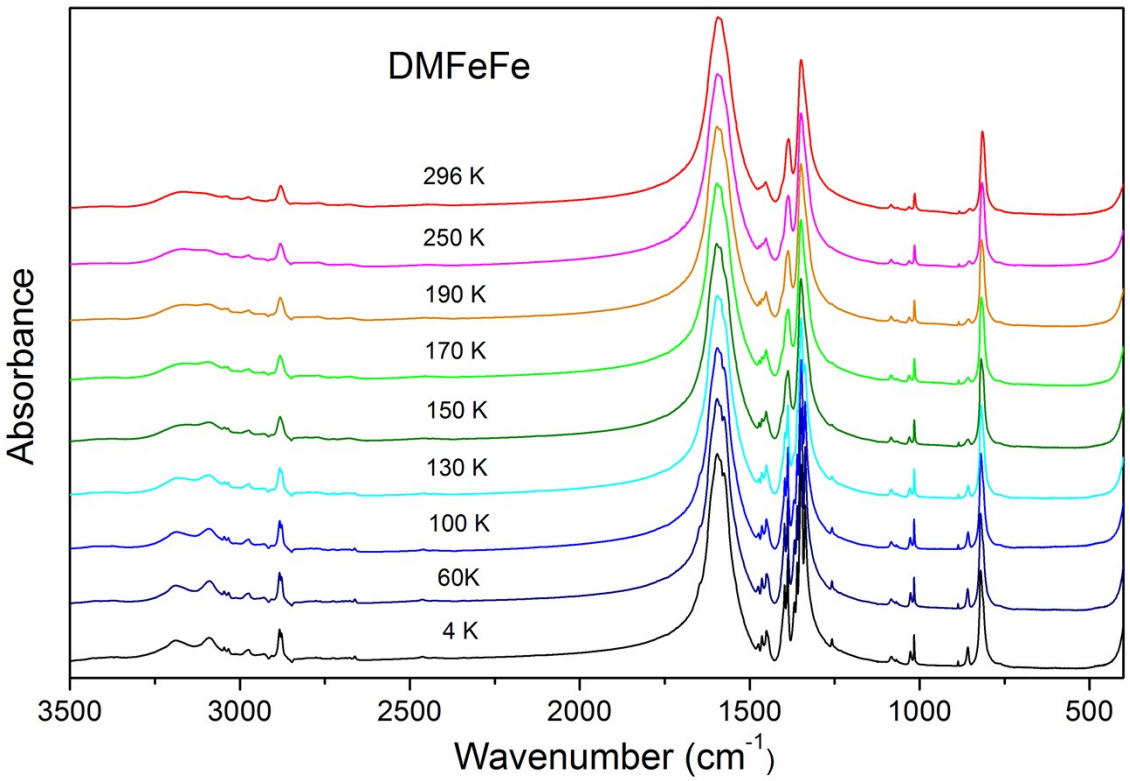

Figure S5. IR spectra of DMFeFe recorded at various temperatures corresponding to the spectral range 400-3500 cm^{-1}.

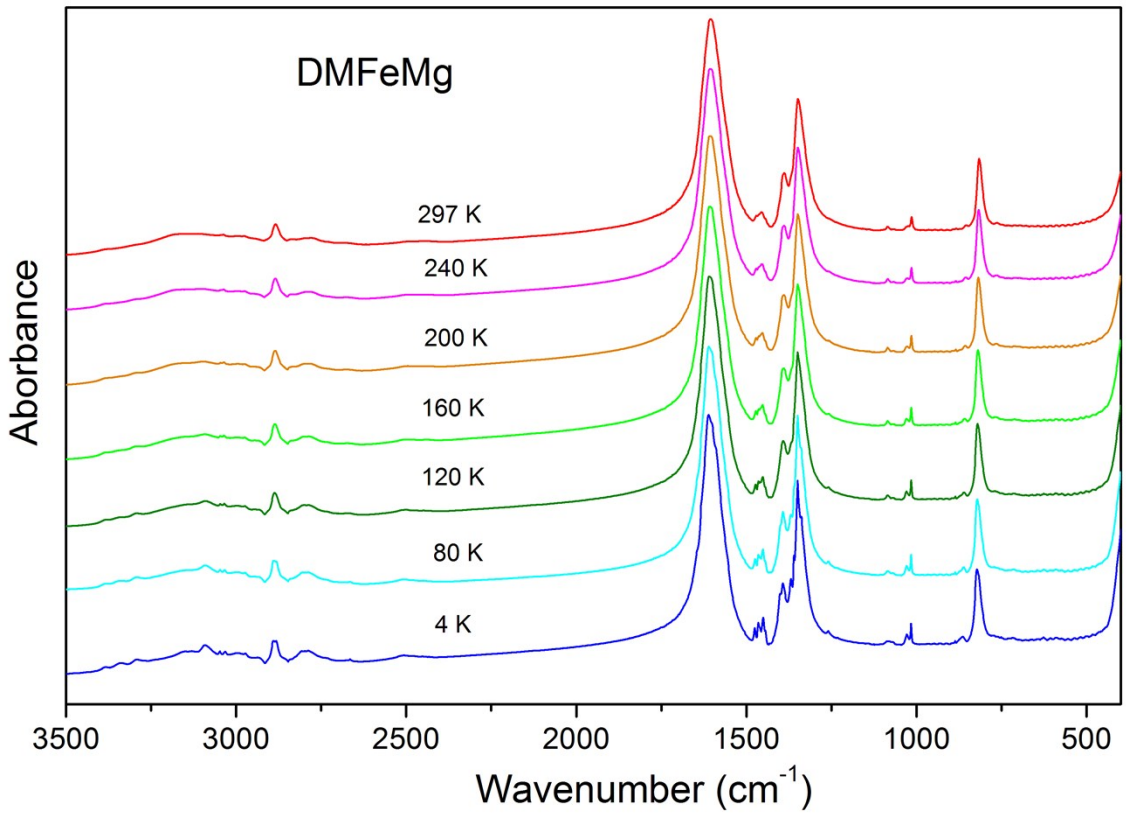

Figure S6. IR spectra of DMFeMg recorded at various temperatures corresponding to the spectral range 400-3500 cm^{-1}.

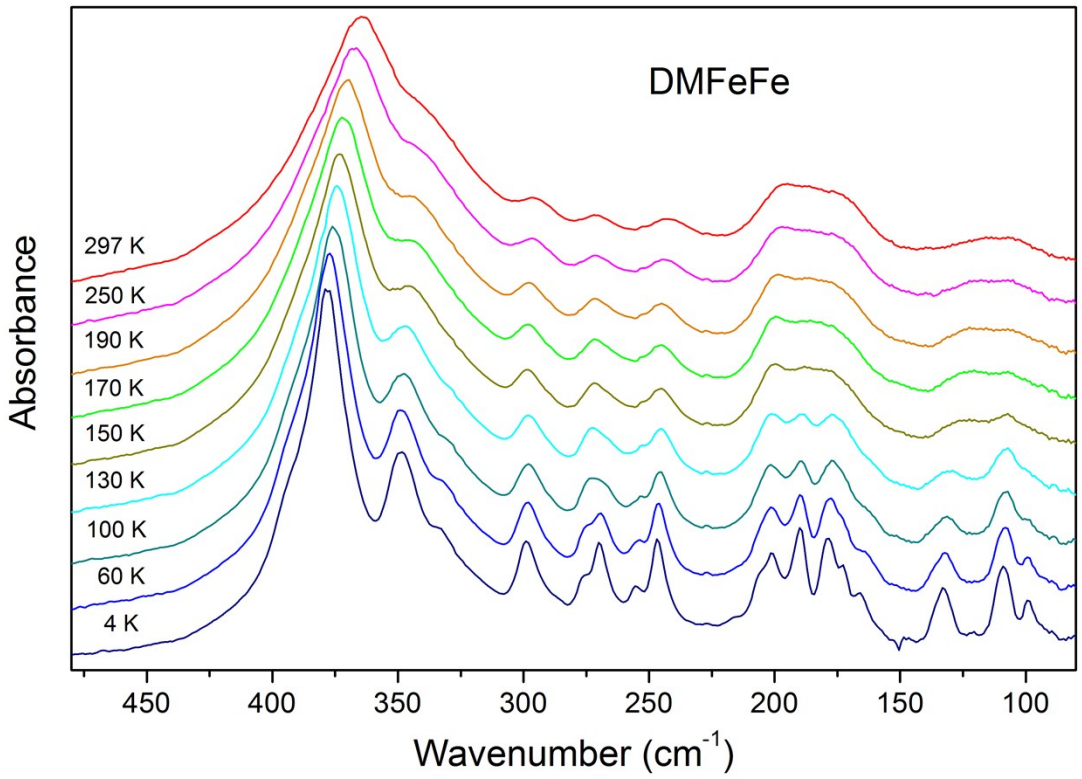

Figure S7. Far-IR spectra of DMFeFe recorded at various temperatures corresponding to the spectral range 80-480 cm^{-1}.

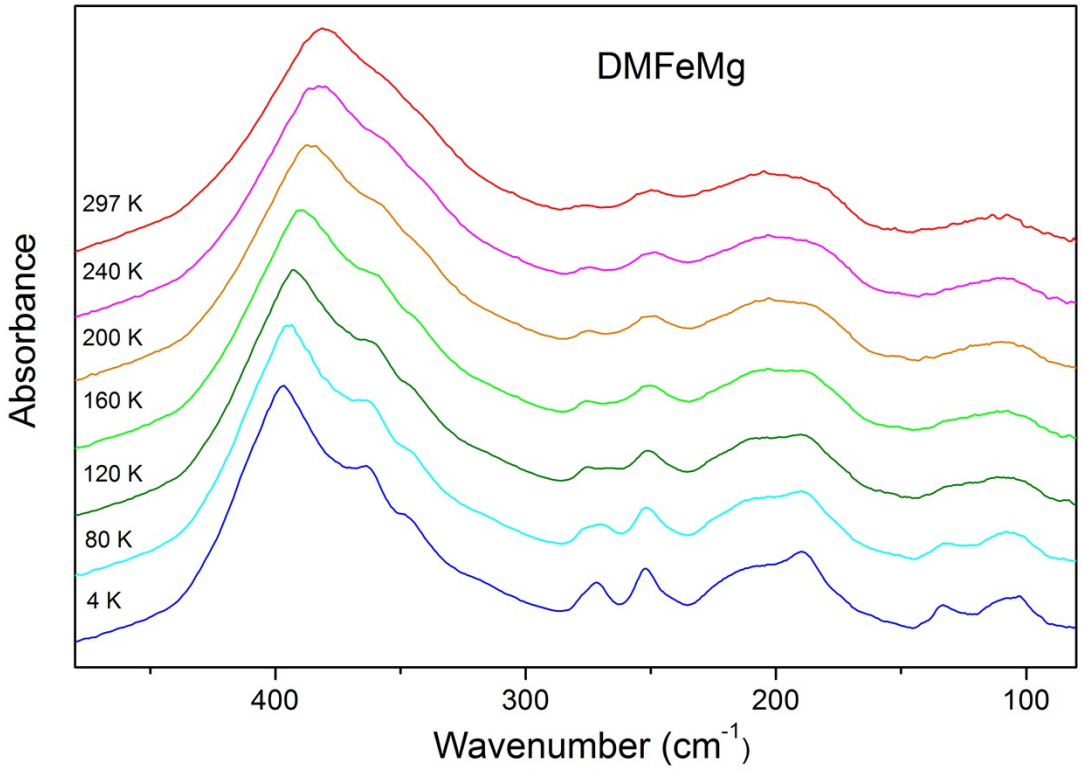

Figure S8. Far-IR spectra of DMFeMg recorded at various temperatures corresponding to the spectral range 80-480 cm^{-1}.

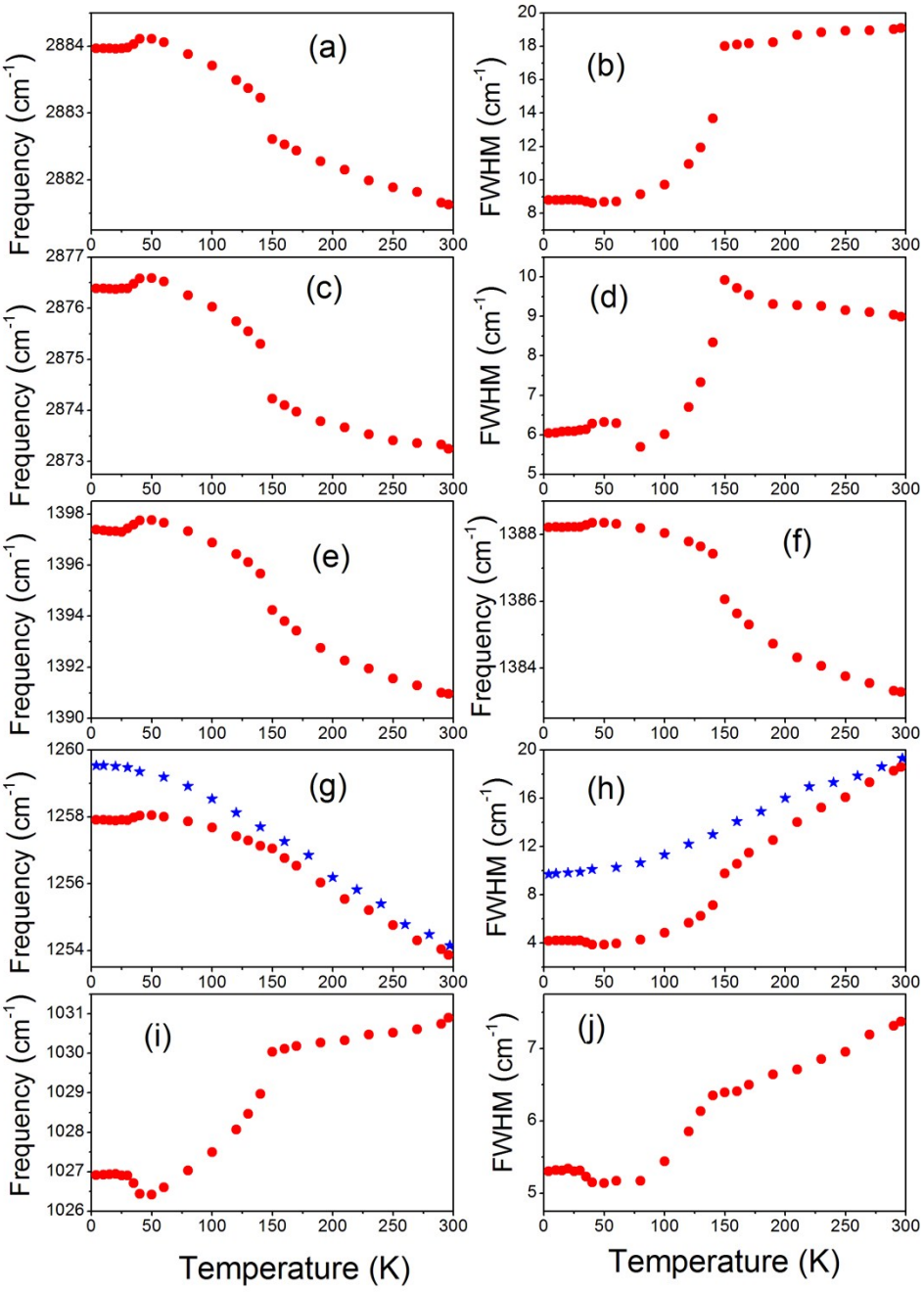

Figure S9. Temperature dependence of IR frequencies for the (a, c) $\nu_1(HCOO^-)$, (e, f) $\nu_5(HCOO^-)$ and (g and i) $\rho(CH_3)$ modes. The corresponding plots of FWHM vs. temperature are shown in (b), (d), (h) and (j) for the 2882, 2873, 1254 and 1031 cm^{-1} IR modes, respectively. Red circles correspond to DMFeFe and blue stars to DMFeMg.

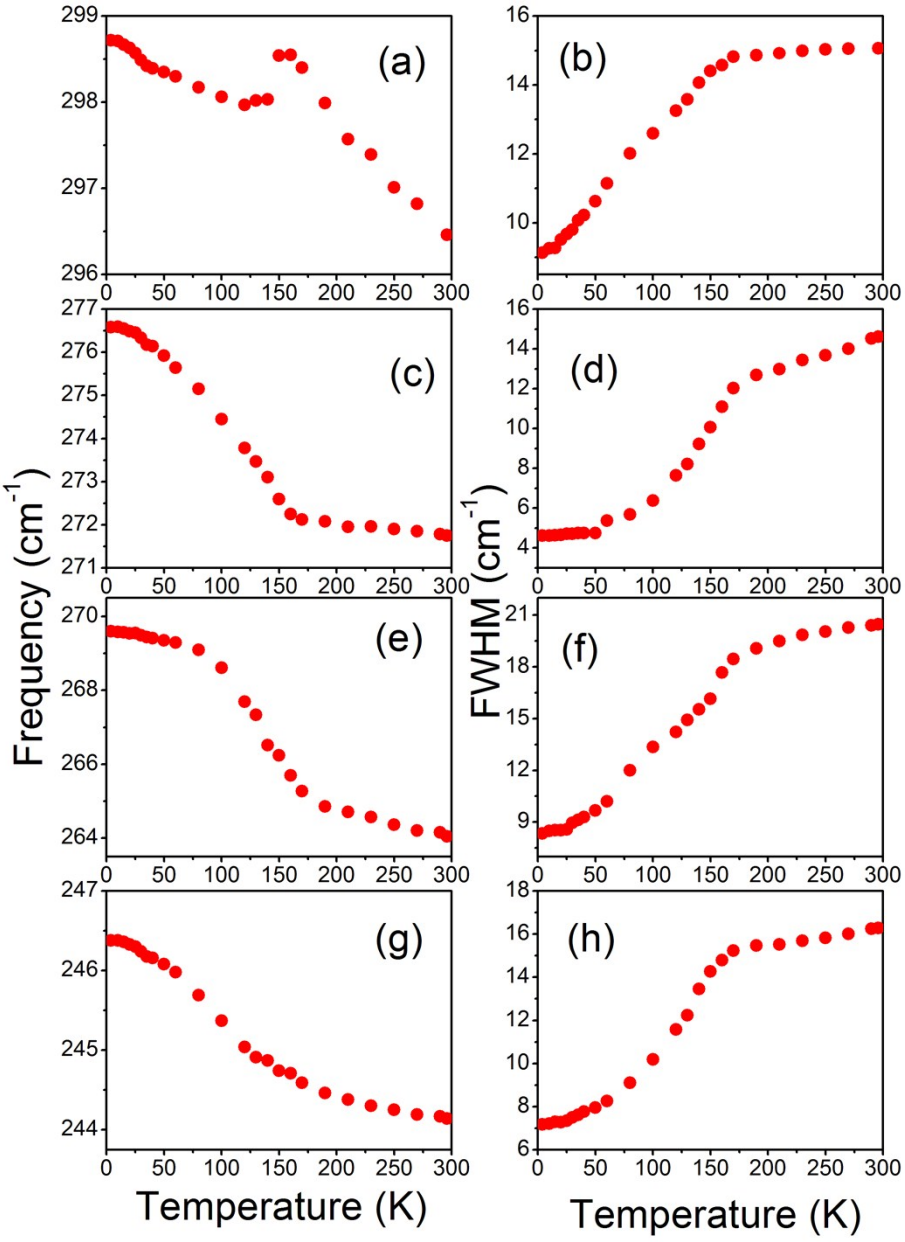

Figure S10. Temperature dependence of IR frequencies for the (a, c, e, g) lattice modes of DMFeFe. The corresponding plots of FWHM vs. temperature are shown in (b), (d), (f) and (g).